

# Predicting internal bond strength of particleboard under outdoor exposure based on climate data: comparison of multiple linear regression and artificial neural network

Ken Watanabe · Hideaki Korai · Yasuhiro Matsushita · Tomoyuki Hayashi

Received: 22 May 2014 / Accepted: 10 November 2014 / Published online: 2 December 2014  
© The Japan Wood Research Society 2014

**Abstract** The internal bond strength (IB) of a commercial particleboard put under various outdoor exposure conditions were modeled using a multiple linear regression (MLR) and an artificial neural network (ANN). The outdoor exposure data used in this study were collected from the results of past outdoor exposure tests conducted at eight locations across Japan from 2004 to 2011. The data from five locations were used to develop the MLR model and the ANN model for predicting the IB of particleboard under outdoor exposure based on climate data including exposure duration, annual mean temperature, annual sunshine duration, and annual precipitation. The performance of the models was assessed by comparing predicted IB values with measured ones for the remaining three locations. The MLR model gave a high  $R^2$  of 0.87 and a low root mean square error (RMSE) of 0.07 MPa, while the ANN model gave an  $R^2$  of 0.93 and an RMSE of 0.05 MPa. Thus, both models were demonstrated to be applicable to particleboards exposed at different locations in Japan. A statistical test of the MLR model revealed that the IB was influenced negatively by exposure duration, temperature, and precipitation. These influences were confirmed by the sensitivity

analysis of the ANN model, and the analysis also showed an additional positive influence of sunshine duration on IB.

**Keywords** Internal bond strength · Particleboard · Outdoor exposure · Artificial neural network · Multiple linear regression

## Introduction

Outdoor exposure test is one of the standard methods for evaluating the durability of wood-based boards. As a test specimen is exposed in a natural weathering environment for a long-term period, the deterioration of the test specimen strongly depends on the climate conditions of the exposure locations. Consequently, the results of the outdoor exposure tests conducted at specific locations are not generally applicable to locations with different climate conditions. This is a disadvantage of outdoor exposure test.

To overcome this problem, Sekino et al. [1] and Kojima et al. [2, 3] extensively collected the outdoor exposure data of commercial wood-based boards exposed at eight representative locations across Japan, and quantified the deterioration of wood-based boards at different locations. The relationships between board deterioration and outdoor exposure conditions were modeled by introducing a combination of climate factors, called “weathering intensity (WI)”. The best combination of climate factors was determined based on the coefficient of correlation from simple linear regression analysis, and it was found that the WI defined by the logarithm of  $\sum (\text{Temperature} \times \text{Precipitation})$  was highly correlated to the deterioration of mechanical properties, namely internal bond strength (IB), modulus of rupture, and lateral nail resistance. Although the WI data were well fitted by the regression analysis, it

K. Watanabe (✉) · H. Korai  
Forestry and Forest Products Research Institute, 1 Matsunosato,  
Tsukuba, Ibaraki 305-8687, Japan  
e-mail: kenwatanabe@ffpri.affrc.go.jp

Y. Matsushita  
SET Software Co., Ltd, 1-7-10 Bingomachi, Chuo-ku,  
Osaka 541-0051, Japan

T. Hayashi  
The Institute of Wood Technology, Akita Prefectural University,  
11-1 Kaiezaka Noshiro, Akita 016-0876, Japan

remains unclear whether the WI is applicable to predict the deterioration of wood-based boards, because no validation was performed with an independent set of data.

Furthermore, there are three questions regarding the data analysis. Firstly, the WI is a combination of climate factors involving mathematical transformation, so it is difficult to examine the impact of individual climate factors on the deterioration of wood-based boards. Secondly, simple linear regression uses one variable to explain patterns in the data by looking for a relationship between two continuous variables. If there is more than one possible explanatory variable and an important third variable is not included, we could miss significant relationships between the first two variables, or even come to the wrong conclusion [4]. Instead, it would then be more efficient to include all the information available in a multivariate analysis. Thirdly, a group of parametric tests, including linear regression, *t* test and analysis of variance (ANOVA), relies on the four assumptions: independence, homogeneity of variance, normality of error, and linearity [4]. If these assumptions are contravened, the parameter estimates are no longer valid and the statistical significance of WI cannot be assessed. It is highly likely that one or more assumptions were contravened by the simple linear regression between the WI and the deterioration of mechanical properties. Therefore, in this paper, we addressed these questions using multiple linear regression (MLR), presenting how to check the assumptions of MLR.

Contrastingly, an artificial neural network (ANN) is a nonlinear computational model, capable of modeling complex, undefined, and nonlinear relationships between variables with better results than traditional statistical regressions [5]. The background information on ANNs can be found in the literatures [6, 7]. The characteristic feature of ANNs is that they are not programmed; they are trained from a series of examples without needing to know beforehand the relations which may exist between the variables involved in the process, by adjusting the weight of the relations between the variables. In the field of wood science, ANNs have been applied to predict mechanical and physical properties of wood [8–10], fracture toughness [11], thermal conductivity [12], hygroscopic equilibrium moisture content [13], nonisothermal diffusion of moisture [14], dielectric loss factor [15], and drying process of wood [16–19]. Also in the field of wood-based composite materials, some mechanical and physical properties of wood-based boards have been successfully predicted using ANNs based on their physical properties [20–24] or based on processing parameters which are to be optimized in a board manufacturing process [25–28].

In this study, we focused on the IB of particleboard subjected to outdoor exposure. An MLR and an ANN were developed to predict the IB of particleboard during outdoor

exposure based on climate data collected at eight locations in Japan. The ANN model and the MLR model were developed with the data from five locations, and the performance of the models was assessed for the remaining three locations. In addition, techniques to check the assumptions in MLR were presented, and the impact of climate exposure on the IB under outdoor exposure was examined by means of statistical analysis.

## Materials and methods

### Samples and outdoor exposure tests

Industry-manufactured phenol–formaldehyde resin-bonded particleboards (hereafter call “board”) were obtained for the experiments. The boards were manufactured from wood processing residues, and satisfied the waterproof category of Type 18 and Type P boards under JIS A-5908 [29]. Type 18 boards satisfy 18 MPa in modulus of rupture, and Type P indicates waterproof particleboard. The density and thickness of the boards were 0.75 g/cm<sup>3</sup> and 12.2 mm. The industry-manufactured boards did not allow revealing the information on the processing parameters, such as particle size, hot pressing temperature, and time. Further details are provided in the references [30, 31]. Thirty specimens measuring 50 × 50 mm were prepared for control, and the IB test was conducted according to JIS-5908 [29]. The initial IB was 0.83 MPa on average with a standard deviation of 0.09 MPa.

The outdoor exposure tests were conducted at eight locations in Japan from February 2004 to March 2011. Figure 1 and Table 1 show the latitude, longitude, and climate conditions of the locations. Twelve particleboards measuring 300 × 300 mm were set up for each location on

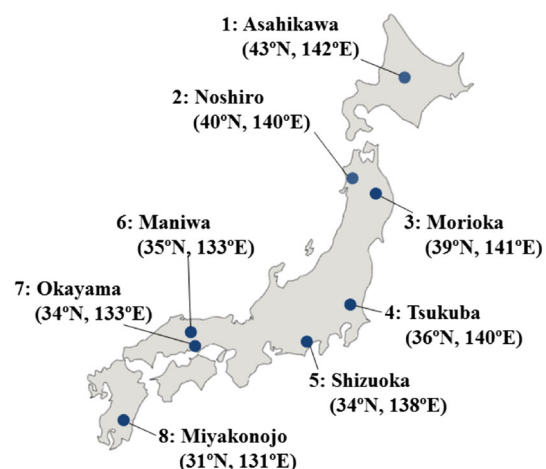


**Fig. 1** Eight locations for outdoor exposure tests in Japan

**Table 1** Summary of  $T_m$ ,  $S_m$ , and  $P_m$  for each location

Location <i>j</i>	$T_m$ (°C)				$S_m$ (h)				$P_m$ (mm)			
	Mean	SD	Max	Min	Mean	SD	Max	Min	Mean	SD	Max	Min
1	7.1	0.1	7.2	7.0	1582.7	21.6	1605.8	1548.5	979.2	21.4	1008.8	945.5
2	11.5	0.1	11.6	11.4	1377.7	66.7	1444.1	1271.6	1554.2	108.7	1731.0	1456.3
3	10.5	0.1	10.6	10.3	1660.8	25.0	1690.8	1632.8	1388.5	93.3	1534.5	1296.4
4	14.3	0.1	14.5	14.2	2043.5	88.1	2173.8	1963.2	1466.4	129.8	1693.0	1377.4
5	17.0	0.2	17.4	16.9	2151.0	64.8	2256.5	2100.3	2576.7	446.0	3453.5	2302.1
6	14.2	0.1	14.5	14.2	1788.4	13.9	1816.3	1780.6	1374.9	153.1	1682.5	1273.7
7	16.7	0.1	16.9	16.7	2046.5	26.1	2083.8	2020.9	1168.5	172.0	1509.0	1056.7
8	16.9	0.1	17.0	16.8	2011.6	27.8	2046.5	1979.7	2746.2	308.8	3302.0	2462.8

SD standard deviation

an exposure stand that faced south at an angle of 90° to the ground. The cut edges of the boards were coated with enamel paint as a waterproof agent prior to outdoor exposure. Two boards were collected from each location after 1, 2, 3, 4, 5, and 6 (or 7) years of exposure, and were subjected to the IB test. Prior to the IB test, the boards were conditioned to the moisture content of approximately 10 %. For each location, thirteen specimens measuring 50 × 50 mm were cut from the boards. The detailed cutting pattern was described by Korai et al. [30, 31].

Data preparation

Climate data of the eight locations for the exposure period were collected from the website of the Meteorological Agency in Japan [32]. The data included annual mean temperature ( $T$ ), annual sunshine duration ( $S$ ), and annual precipitation ( $P$ ). The individual annual data were averaged over exposure period ( $t$ ;  $t = 1-7$  years) using the following equations:

$$T_{mj} = \frac{1}{t} \sum_{k=1}^t T_{kj} \quad (t = 1-7, j = 1-8) \tag{1}$$

$$S_{mj} = \frac{1}{t} \sum_{k=1}^t S_{kj} \quad (t = 1-7, j = 1-8) \tag{2}$$

$$P_{mj} = \frac{1}{t} \sum_{k=1}^t P_{kj} \quad (t = 1-7, j = 1-8) \tag{3}$$

where  $j$  is the location number,  $T_{mj}$  is the mean  $T$  of the location  $j$  during the exposure period  $t$ ,  $S_{mj}$  is the mean  $S$  of the location  $j$  during the exposure period  $t$ ,  $P_{mj}$  is the mean  $P$  of the location  $j$  during the exposure period  $t$ . Table 1 lists a summary of the mean annual climate data for each location.

The IB values of the thirteen specimens obtained from the same location were averaged to remove the variability in IB between the specimens. The mean IB ( $IB_m$ ) of each

location is shown in Fig. 2 providing strong evidence that the IB deterioration depended on the exposure duration and the climate conditions at each location.

The data obtained from the eight locations were separated into two groups by analyzing the variability in the climate data of each location, as discussed later in the results and discussion section. The data from the locations 1, 2, 4, 7, and 8 were used to develop MLR and ANN models, while the data from the remaining three locations 3, 5, and 6 were used to evaluate the predictive ability of the models.

MLR model

We considered models that assume the IB deterioration of particleboard under outdoor exposure was influenced by exposure period, temperature, sunshine duration, and precipitation. An MLR model was developed assuming that  $IB_m$  depends linearly on  $t$ ,  $T_m$ ,  $S_m$ , and  $P_m$ . The developed MLR model was expressed as following:

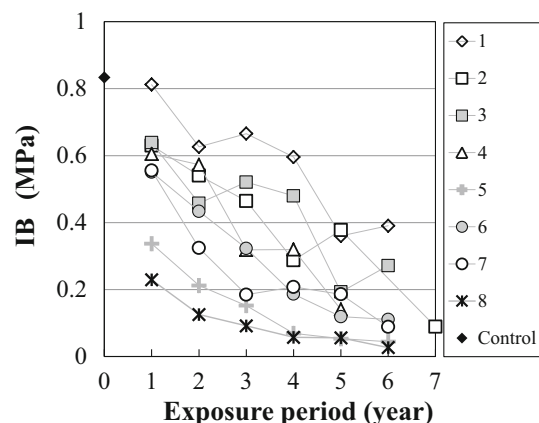


**Fig. 2** Mean internal bond strength (IB) of each location as a function of exposure period

$$IB_m = \beta_0 + \beta_1 \times t + \beta_2 \times T_m + \beta_3 \times S_m + \beta_4 \times P_m + \varepsilon \quad (4)$$

where  $\beta_i$  ( $i = 0-4$ ) represent parameters to be estimated, and  $\varepsilon$  is the error term following a normal distribution with a mean zero and constant variance.

The assumptions of MLR, such as homogeneity of variance, normality of error, and linearity, were diagnosed by looking for patterns in certain plots [4]: standardized residual plots against fitted values and quantile–quantile plot ( $Q-Q$  plot) against normal distribution. In addition, the variance inflation factor (VIF) was used to assess the levels of multicollinearity. VIFs measure how much the variances of the estimated regression coefficients are inflated as compared to when the predictor variables are not linearly related. VIFs larger than 5–10 imply problems with multicollinearity between input variables, which can lead to models with poor prediction [33]. The analysis of MLR was performed using R, version 3.0.1 [34].

#### ANN model

An ANN model was constructed to predict  $IB_m$  using NeuralWorks Predict (NWP) software (NeuralWare Inc., Pittsburgh, PA, USA). The input variables were  $t$ ,  $T_m$ ,  $S_m$ , and  $P_m$ , while the output layer was  $IB_m$ . The input variables were nonlinearly transformed to avoid complex representation of the model. A genetic algorithm [35] was employed to make a suitable choice of input variables from the set of all input variables and transformations of input variables [36]. The types of transformation selected included the linear, square, and hyperbolic tangent, whereupon ANNs were constructed by a cascade-correlation learning algorithm [37]. The cascade-correlation is a method of incrementally adding processing elements. Instead of adjusting the weights in an ANN of fixed topology, cascade-correlation begins with a minimal network, then automatically trains and adds new hidden units one by one, creating a multilayer structure. Once a new hidden unit has been added to the ANN, its input-side weights are frozen. This unit then becomes a permanent feature detector in the ANN, available for producing outputs or creating other, more complex feature detectors. The flowchart of the ANN modeling is depicted in Fig. 3.

To show the degree of contribution of the input variables to the determination of the network output, a sensitivity analysis was performed with NWP that computes partial derivatives of the output variable with respect to each of the input variables. The sensitivity analysis produces a quantitative measure of the variation in the  $IB_m$  calculated by the network, when each variable changes. The normalized sensitivity for each input variable was calculated according to Eq. (5):

$$\text{Normalized sensitivity} = \frac{\sum_{i=1}^N \left( \frac{\partial y_i}{\partial x_i} \right)^2}{\sigma^2 N} \quad (5)$$

where  $\sigma^2$  is the variance of the partial derivatives for each input variable,  $x_i$  and  $y_i$  are the input and output vectors for each data set. High values of this sensitivity indicate that a slight variation of the variable produces considerable changes in the output  $IB_m$ , and vice versa. Furthermore, the average value of sensitivity for each input variable was calculated according to Eq. (6):

$$\text{Average value of sensitivity} = \frac{\sum_{i=1}^N \frac{\partial y_i}{\partial x_i}}{N} \quad (6)$$

which indicates a positive relationship between input and output variables for its positive sign, while a negative sign indicates an inverse relationship. This is a standard diagnostic procedure commonly used to gain insight into a multilayer neural network solution [36].

## Results and discussion

### Climate variability between locations

Principal component analysis was employed for the climate variables, namely  $T_m$ ,  $S_m$ , and  $P_m$ , so that the climate variability between locations could be observed in the two-dimensional score plot (Fig. 4). It is clear that the locations 5 and 8 are clustered in the top right-hand corner, indicating that the climate conditions at locations 5 and 8 are different from those at the other locations. These two locations had relatively high  $T_m$  and  $P_m$  (Table 1), and showed the lowest  $IB_m$  among the eight locations over the entire exposure period (Fig. 2), whereas the location 1 in the bottom left-hand corner had the lowest  $T_m$  and  $P_m$ , and showed the highest  $IB_m$ . Therefore, the score plot shows the tendency of IB deterioration in association with climate conditions. Kojima et al. [2, 3] geographically divided eight locations into northern Japan (location 1–4) and southern Japan (location 5–8), and the IB deterioration was evaluated for each group separately. This geographical difference is apparently reflected on the first principal component in Fig. 4.

If the data for model construction are collected from the locations with similar climate condition, the model will not be applicable to the external locations with different climate conditions. The climate variability between locations was checked by the score plot, and the eight locations were divided to avoid substantial bias between groups. Consequently, the locations 1, 2, 4, 7, and 8 were selected for model development, while the data from the remaining

**Fig. 3** Flowchart of the ANN modeling.  $t$  exposure period,  $T$  annual mean temperature,  $S$  annual sunshine duration,  $P$  annual precipitation,  $IB$  internal bond strength

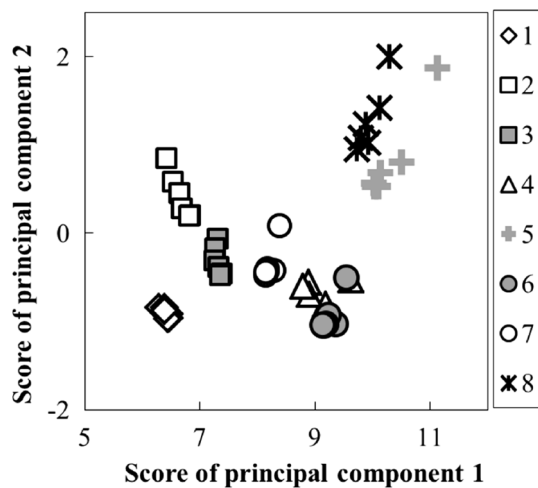
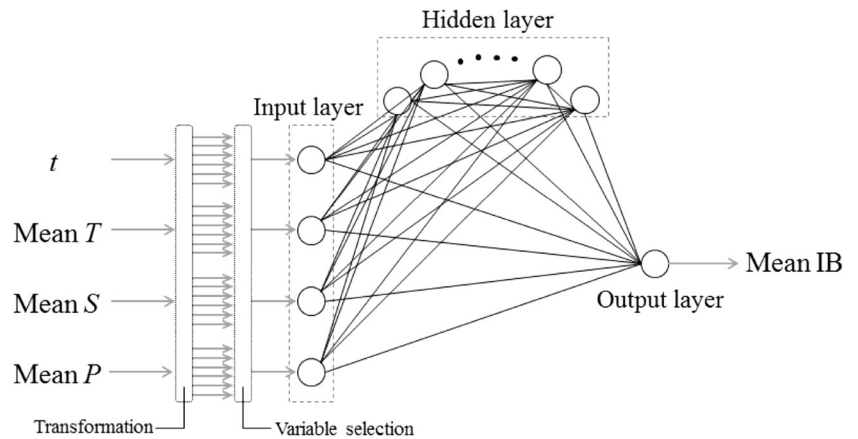


**Fig. 4** Score plot for the first two principal components. The individual plots represent locations for each exposure period  $t$

three locations (3, 5, and 6) were used to evaluate the predictive ability of the models.

Checking assumptions of MLR

An important aspect of regression involves assessing the tenability of the assumptions upon which its analyses are based. The assumption of independence of observations, which is fundamental to all statistics, was fulfilled at the design stage of this study.

The residuals from the model were examined to check the assumptions of linearity and homogeneity of variance. In Fig. 5, the standardized residuals were more or less evenly scattered above and below their mean of zero, indicating that the data satisfied both assumptions.

The normality assumption was assessed through normal  $Q-Q$  plot in Fig. 6. The displayed points should follow a linear shape if the data values are from normal distribution. The  $Q-Q$  plot shows that the residuals were approximately

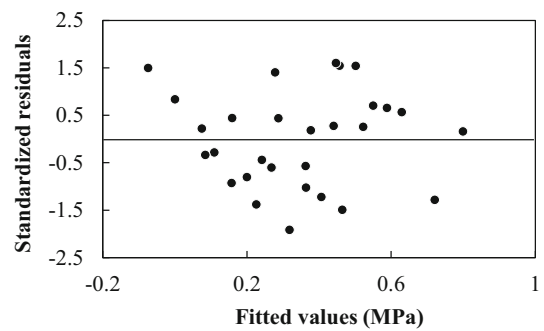


**Fig. 5** Plots of fitted values versus standardized residuals

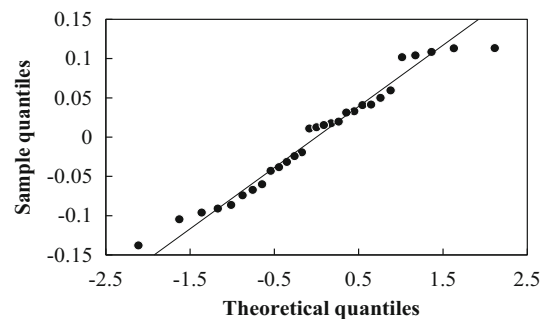


**Fig. 6** Normal quantile–quantile plots. The *solid line* is the line that goes through the 25th and 75th percentiles of the data and of the theoretical distribution

normally distributed, since the plots did not depart from the expected identity line. These results confirm that the data satisfied the assumptions of MLR.

Interpretation of MLR model

The results of type II ANOVA for the MLR model is listed in Table 2. The inspection of the ANOVA table suggests that  $t$ ,  $T_m$ , and  $P_m$  were significant factors of  $IB$  giving  $p < 0.05$ . This finding supports the fact that the  $WI$  (the

**Table 2** Type II ANOVA table for MLR model

	SS	df	F value	P value
$t$	0.9213	1	171.15	$2.20 \times 10^{-16}$
$T_m$	0.1729	1	32.11	$1.20 \times 10^{-6}$
$S_m$	0.0009	1	0.17	$6.85 \times 10^{-1}$
$P_m$	0.0709	1	13.17	$0.77 \times 10^{-3}$
Residuals	0.2261	42		

SS sums of squares,  $df$  degree of freedom

logarithm of the sum of ( $T \times P$ ) over exposure period) was highly correlated to IB [2, 3]. The sums of squares and  $F$  value were highest for  $t$ , followed by  $T_m$  and  $P_m$  in decreasing order. Therefore, the exposure period was found to be the most influential factor on IB deterioration, followed by  $T_m$  and  $P_m$ .

In contrast,  $S_m$  was insignificant ( $p = 0.685$ ), indicating that sunshine duration had little influence on IB deterioration of particleboard under outdoor exposure. This finding is consistent with the suggestion that sunlight does not directly affect the internal deterioration of board and that IB is an interior property of boards [2].

Variance inflation factor was used to measure collinearity among explanatory variables. The VIF values were lower than 5 for all variables, indicating the absence of multicollinearity. The estimated coefficient for  $S_m$  was zero, and as a result, the developed MLR was expressed as following;

$$IB_m = 1.1521 - 0.0841 \times t - 0.0340 \times T_m - 0.0009 \times P_m \quad (7)$$

The coefficients for all variables showed negative values, and the MLR model gave an  $R^2$  of 0.89 (adjusted  $R^2$  of 0.88). This means that 88–89 % of the  $IB_m$  variance could be explained by the linear model assuming that exposure duration, temperature, and precipitation negatively affect IB in an additive manner. These results demonstrate that the MLR model was useful to assess the impact of climate on IB of particleboard under outdoor exposure. It is, however, noted that the MLR model is applicable within the limited exposure period of this study, as discussed later.

#### Interpretation of ANN model

The architecture of the ANN model consisted of 4 input neurons, 9 neurons with a hyperbolic tangent transfer function in the hidden layer, and 1 output neuron with a sigmoid transfer function. To estimate the relative importance of the individual climate variables to model predictions, the normalized sensitivity was calculated for each

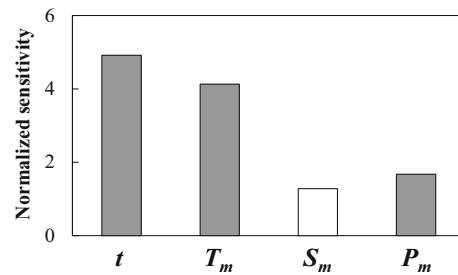


**Fig. 7** Results of sensitivity analysis in the ANN model. Gray bars represent average sensitivity  $< 0$ ; white bars represent average sensitivity  $> 0$

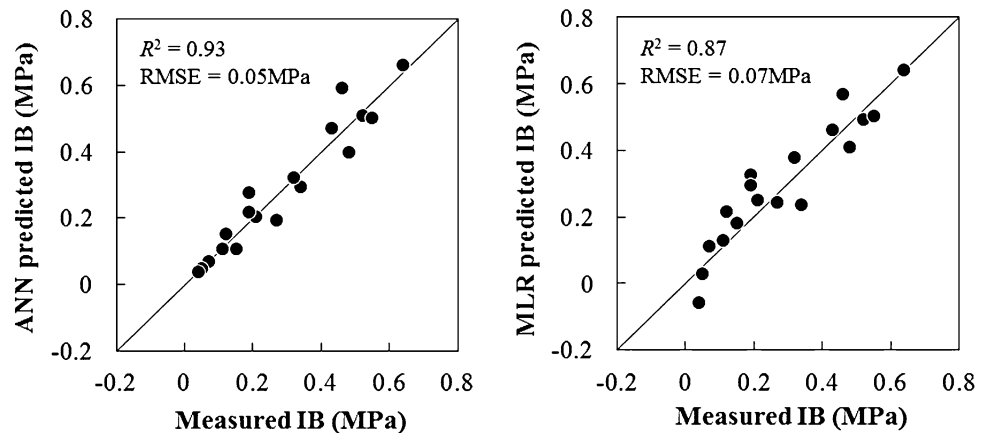
input variable (Fig. 7). It is apparent that  $t$ ,  $T_m$ , and  $P_m$  had a negative influence, and  $t$  was the variable presenting a higher impact on  $IB_m$ , followed by  $T_m$  and  $P_m$ . This order is consistent with the results of the MLR model. Conversely,  $S_m$  had a relatively small and positive impact on  $IB_m$ . It is likely to reflect the nonlinear relationships between  $S_m$  and  $IB_m$ , which was not found in the statistical test of the MLR model. Although  $S_m$  does not directly affect the internal deterioration of board, solar radiation facilitates the evaporation of rain water from the surface and prevents water from penetrating into the interior of board. This may be a reasonable explanation for the positive impact of  $S_m$ .

#### Predictive ability of ANN model and MLR model

Figure 8 shows the plots of the experimentally measured versus predicted  $IB_m$  using the ANN model and MLR model, respectively. The ANN model gave an  $R^2$  of 0.93 and a root mean square error (RMSE) of 0.05 MPa, while the MLR model gave an  $R^2$  of 0.87 and an RMSE of 0.07 MPa. Thus, the predictive ability of both models was good, and they were demonstrated to be robust and applicable to boards exposed at different locations in Japan.

The ANN model gave a higher  $R^2$  and a lower RMSE than the MLR model. Therefore, the ANN model outperformed the MLR model for predicting  $IB_m$ . As can be seen in the Eq. (7), the MLR model assumes that  $IB_m$  decreases by 0.0841 MPa per year, independent from the magnitude of  $IB_m$ . Consequently, in Fig. 8, the MLR model showed a negative value when its measured IB value was close to zero. It is concerned that MLR will be vulnerable when the exposure period is further increased and the boards continue degrading, because the assumption of linearity will no longer be valid. In contrast, ANN is capable of describing nonlinear effects of climate variables without any assumptions. This flexibility of ANN makes it more suitable for predicting the IB of particleboard under outdoor exposure.

**Fig. 8** Plots of the experimentally measured versus predicted IB using the ANN model (left) and the MLR model (right). The solid line represents a one-to-one relationship between measured and predicted values



## Conclusion

The IB deterioration of a commercial particleboard put under various outdoor exposure conditions were examined by developing the MLR model and the ANN model based on climate data including exposure duration, annual mean temperature, annual sunshine duration, and annual precipitation. Our results showed that both the models could be used to predict the IB of Type 18 and Type P particleboards exposed at different locations in Japan, and that the ANN model yielded slightly better performance than the MLR model.

It should be noticed that the MLR is based on the four assumptions: independence, homogeneity of variance, normality of error, and linearity. It is important to check the assumptions that we made in fitting the data. If these assumptions are contravened, the significance levels are no longer valid and the worth of the whole analysis is cast into doubt. In contrast, ANNs allow for flexible modeling of both linear and nonlinear behavior of IB deterioration without any assumptions that are required for MLR. Therefore, the ANNs are considered to be more suitable to predict the IB of particleboard under outdoor exposure.

**Acknowledgments** This study was partially supported by Research grant No. 201207 of Forestry and Forest Products Research Institute. Outdoor exposure tests were conducted at eight locations in Japan as part of a project organized by the Research Working Group on Wood-based Boards from the Japan Wood Research Society. The authors thank all participants in this project.

## References

1. Sekino N, Sato H, Adachi K (2014) Evaluation of particleboard deterioration under outdoor exposure using several different types of weathering intensity. *J Wood Sci* 60:141–151
2. Kojima Y, Shimoda T, Suzuki S (2012) Modified method for evaluating weathering intensity using outdoor exposure tests on wood-based panels. *J Wood Sci* 58:525–531
3. Kojima Y, Shimoda T, Suzuki S (2011) Evaluation of the weathering intensity of wood-based panels under outdoor exposure. *J Wood Sci* 57:408–414
4. Grafen A, Hails R (2002) *Modern statistics for the life sciences*. Oxford University Press, Oxford
5. Sukthomya W, Tannock A (2005) The training of neural networks to model manufacturing processes. *J Intell Manuf* 16:39–51
6. Picton P (2000) *Neural networks*, 2nd edn. Palgrave, New York
7. Samarasinghe S (2006) *Neural networks for applied sciences and engineering. From fundamentals to complex pattern recognition*. CRC Press, Boca Raton
8. Mansfield SD, Iliadis L, Avramidis S (2007) Neural network prediction of bending strength and stiffness in western hemlock (*Tsuga heterophylla* Raf.). *Holzforschung* 61:707–716
9. Mansfield SD, Kang K-Y, Iliadis L, Tachos S, Avramidis S (2011) Predicting the strength of *Populus* spp. clones using artificial neural networks and  $\epsilon$ -regression support vector machines ( $\epsilon$ -rSVM). *Holzforschung* 65:855–863
10. Esteban LG, Fernández FG, de Palacios P (2009) MOE prediction in *Abies pinsapo* Boiss. timber: application of an artificial neural network using non-destructive testing. *Comp Struct* 87:1360–1365
11. Samarasinghe S, Kulasiri D, Jamieson T (2007) Neural networks for predicting fracture toughness of individual wood samples. *Silva Fennica* 41:105–122
12. Avramidis S, Iliadis L (2005) Predicting wood thermal conductivity using artificial neural networks. *Wood Fiber Sci* 37:682–690
13. Avramidis S, Iliadis L (2005) Wood-water sorption isotherm prediction with artificial neural networks: a preliminary study. *Holzforschung* 59:336–341
14. Avramidis S, Wu H (2007) Artificial neural network and mathematical modeling comparative analysis of nonisothermal diffusion of moisture in wood. *Holz Roh Werkstoff* 65:89–93
15. Avramidis S, Iliadis L, Mansfield SD (2006) Wood dielectric loss factor prediction with artificial neural networks. *Wood Sci Technol* 40:563–574
16. Wu H, Avramidis S (2006) Prediction of timber kiln drying rates by neural networks. *Dry Technol* 24:1541–1545
17. Ceylan I (2008) Determination of drying characteristics of timber by using artificial neural networks and mathematical models. *Dry Technol* 26:1469–1476
18. Watanabe K, Matsushita Y, Kobayashi I, Kuroda N (2013) Artificial neural network modeling for predicting final moisture content of individual Sugi (*Cryptomeria japonica*) samples during air-drying. *J Wood Sci* 59:112–118

19. Watanabe K, Kobayashi I, Matsushita Y, Saito S, Kuroda N, Noshiro S (2014) Application of near-infrared spectroscopy for evaluation of drying stress on lumber surface: a comparison of artificial neural networks and partial least-squares regression. *Dry Technol* 32:590–596
20. Fernández FG, Esteban LG, de Palacios P, Navarro N, Conde M (2008) Prediction of standard particleboard mechanical properties utilizing an artificial neural network and subsequent comparison with a multivariate regression model. *Invest Agrar Sist Recur For* 17:178–187
21. Fernández FG, de Palacios P, Esteban LG, Garcia-Iruela A, Rodrigo BG, Menasalvas E (2012) Prediction of MOR and MOE of structural plywood board using an artificial neural network and comparison with a multivariate regression model. *Comps B* 43:3528–3533
22. Esteban LG, Fernández FG, de Palacios P, Conde M (2009) Artificial neural networks in variable process control: application in particleboard manufacture. *Invest Agrar Sist Recur For* 18:92–100
23. Esteban LG, Fernández FG, de Palacios P, Rodrigo BG (2010) Use of artificial neural networks as a predictive method to determine moisture resistance of particle and fiber boards under cyclic testing. *Wood Fiber Sci* 42:335–345
24. Esteban LG, Fernández FG, de Palacios P (2011) Prediction of plywood bonding quality using an artificial neural network. *Holzforschung* 65:209–214
25. Cook DF, Chiu CC (1997) Predicting the internal bond strength of particleboard, utilizing a radial basis function neural network. *Eng Appl Artif Intell* 13:171–177
26. André N, Cho H-W, Baek SH, Jeong M-K, Young TM (2008) Prediction of internal bond strength in a medium density fiberboard process using multivariate statistical methods and variable selection. *Wood Sci Technol* 42:521–534
27. Özsahin Ş (2012) The use of an artificial neural network for modeling the moisture absorption and thickness swelling of oriented strand board. *BioResources* 7:1053–1067
28. Ozsahin S (2013) Optimization of process parameters in oriented strand board manufacturing with artificial neural network analysis. *Eur J Wood Prod* 71:769–777
29. JIS A-5908 (2003) JIS standard specification for particleboard. Japanese Standards Association, Tokyo
30. Korai H, Sekino N, Saotome H (2012) Effects of outdoor exposure angle on the deterioration of wood-based board properties. *Forest Prod J* 62:184–190
31. Korai H, Adachi K, Saotome H (2013) Deterioration of wood-based boards subjected to outdoor exposure in Tsukuba. *J Wood Sci* 59:24–34
32. Japan Meteorological Agency website. <http://www.jma.go.jp/jma/indexe.html>. Accessed 18 Dec 2013
33. Montgomery DC, Peck EA (1992) Introduction to linear regression analysis, 2nd edn. Wiley, New York
34. R Core Team (2013) R: a language and environment for statistical computing. R Foundation for Statistical Computing, Vienna. <http://www.R-project.org/>. Accessed 12 Nov 2014
35. Cook DF, Ragsdale CT, Major RL (2000) Combining a neural network with a genetic algorithm for process parameter optimization. *Eng Appl Artif Intell* 13:391–396
36. NeuralWare (2009) NeuralWorks Predict® User Guide. The complete solution for neural data modeling. NeuralWare, Pittsburgh
37. Fahlman SE, Lebiere C (1990) The cascade-correlation learning architecture. Technical Report CMU-CS-90-100. School of Computer Science, Carnegie Mellon University, Pittsburgh